Nuclear magnetic resonance investigation of Li+-ion dynamics in the perovskite fast-ion conductor Li3xLa2/3-x1/3-2xTiO3

2002 J. Phys.: Condens. Matter 14 523

(http://iopscience.iop.org/0953-8984/14/3/321)

INSTITUTE OF PHYSICS PUBLISHING JOURNAL OF PHYSICS: CONDENSED MATTER

J. Phys.: Condens. Matter **14** (2002) 523–539 PII: S0953-8984(02)27038-1

Nuclear magnetic resonance investigation of Li^+-ion dynamics in the perovskite fast-ion conductor $Li_{3x}La_{2/3-x}\square_{1/3-2x}TiO_3$

J Emery[1,4], O Bohnké[2], J L Fourquet[2], J Y Buzaré[1], P Florian[3] and D Massiot[3]

[1] Laboratoire de Physique de l'Etat Condensé (UMR 6087 CNRS), Université du Maine, Avenue O Messiaen, 72085 Le Mans Cédex 9, France
[2] Laboratoire des Fluorures (UMR 6010 CNRS), Université du Maine, Avenue O Messiaen, 72085 Le Mans Cédex 9, France
[3] Centre de Recherche sur les Matériaux à Hautes Températures, CNRS 45071, Orléans Cédex 2, France

E-mail: joel.emery@univ-lemans.fr

Received 20 July 2001, in final form 31 October 2001
Published 21 December 2001
Online at stacks.iop.org/JPhysCM/14/523

Abstract

^{7}Li nuclear magnetic resonance relaxation times T_1, $T_{1\rho}$ and T_2 versus temperature are reported in the 150–900 K temperature range for the lithium lanthanum titanate $Li_{3x}La_{2/3-x}\square_{1/3-2x}TiO_3$ perovskite-type fast-ionic conductors. The presence of Li^+ ions of two kinds with slightly differing environments is displayed in these experiments. These ions exhibit two different motions: a fast one with a characteristic frequency around 100 MHz at 350 K and a slow one whose frequency is around 60 kHz at 280 K. These two different Li^+ species cannot be differentiated by means of the fast motion (only one T_1 is observed from the experiments), but only by means of the slow ones (two $T_{1\rho}$ and two T_2 are observed). These motions are respectively attributed to Li^+ motion inside the A-cage of the perovskite structure formed by the oxygen ions and to Li^+ hops between the cages. T_1- and $T_{1\rho}$-studies also performed on the ^{6}Li nucleus clearly show that just dipolar nuclear interaction is responsible for Li^+ relaxation. This result is at variance with what has been previously put forward for the relaxation process in these compounds.

1. Introduction

The compounds belonging to the solid-solution series $(Li_{3x}La_{2/3-x}\square_{1/3-2x})TiO_3$, with $0.06 < x < 0.14$ (hereafter called LLTO), display among the highest ionic conductivities found up to now in the literature for crystalline oxides, i.e. about 10^{-3}–10^{-4} S cm^{-1} at room

[4] Author to whom any correspondence should be addressed.

temperature (RT) [1, 2]. Robertson *et al* [3] and Fourquet *et al* [4] published structural data on the whole composition range. These authors agree in stating that a pure solid solution exists over the composition range $0.06 < x < 0.14$. Furthermore, Fourquet *et al* have shown by means of x-ray diffraction and HREM (high-resolution electron microscopy) that these compounds are disordered crystalline materials. The structural model, obtained from the x-ray diffraction powder pattern analysis and based on the $P4/mmm$ space group, consists of a tetragonal distortion of the cubic ABO_3 perovskite unit cell with $a = b \approx 3.87$ Å and $c \approx 2a$, with a $c/2a$ distortion which decreases with increasing lithium content [4]. Figure 1 shows a schematic view of the unit cell with the TiO_6 octahedra and the A-cages formed by 12 oxygen ions belonging to eight different octahedra. Two kinds of disorder have been mentioned in this study. One disorder type is characterized by the random distribution of La^{3+} ions and vacancies among the sites 1a (0, 0, 0) and 1b (0, 0, 1/2) of the structure. The 1a sites are mainly occupied by La^{3+} ions (around 90% of site occupancy) although the 1b sites are much less frequently occupied by these ions (around just 30% of site occupancy). This disorder implies doubling of the *c*-axis. Another disorder type exists in the stacking of the 1a (La^{3+}-rich) and 1b (La^{3+}-poor) layers, leading to antiphase domains. This disorder results in a broadening of the (h, k, l) peaks of the x-ray diffraction patterns, with $l = 2n + 1$, which we called superstructure lines [4].

The structural model based on the $P4/mmm$ space group seems at the present time to be the best one for describing the structure and it has therefore been chosen for the discussion in this paper. According to this structural model, La^{3+} and vacancies occupy the centres of the perovskite A-cage. Although all authors agree about this La^{3+} location, the location of the Li^+ ions is still a matter of debate. It has been found by recent bond-valence-sum (BVS) calculations [5] that the Li^+ ion is displaced off centre in the A-cage into a distorted tetrahedral coordination. The small radius of this ion also corroborates this result. A discussion about the other proposed models can be found in [5, 6].

It is widely accepted that dc conductivity implies the passage of Li^+ ions from one A-cage to the next vacant one through a bottleneck made of four oxygen ions. The distance between the centres of these ions is 3.8–4.0 Å, leaving enough room for the Li^+ ion to pass through. Several papers dealing with dc-conductivity measurements of LLTO have already been published [1, 2, 7–12]. It has been shown that for temperatures lower than 200 K, the conductivity is thermally activated with an activation energy of 0.20 eV [12]. For higher temperatures, the dc conductivity is thermally assisted [9, 12], as generally observed in both crystalline superionic conductors with disorder in the cation sublattice [13] and in glassy materials [14].

Nuclear magnetic resonance (NMR) studies in the 150–900 K temperature range were performed. Some results have already been published [15–19]. The activation energy obtained from relaxation time T_1-data using the simple Bloembergen–Purcell–Pound (BPP) model led to a result of 0.12 eV at low temperatures [15]. This result was much lower than the activation energy obtained by dc-conductivity experiments [8–12]. This result, which is generally encountered in conductors, can be ascribed to one or several of the following reasons:

(i) NMR is sensitive to dimensionality, unlike dc conductivity;
(ii) NMR studies are performed at 116 MHz while the σ_{dc}-regime is found to be below 1 MHz at 300 K in our experiments exploring different timescales;
(iii) NMR probes ionic local motion while σ_{dc} probes charge-carrier long-range motion, thus probing different length scales.

Thus, the aim of this paper is to cast light on the dynamics of the Li^+ ions in the LLTO structure by using NMR. It is essentially devoted to the presentation, analysis and discussion of experimental NMR data, from either static spectra or the relaxation times T_1, $T_{1\rho}$ and T_2

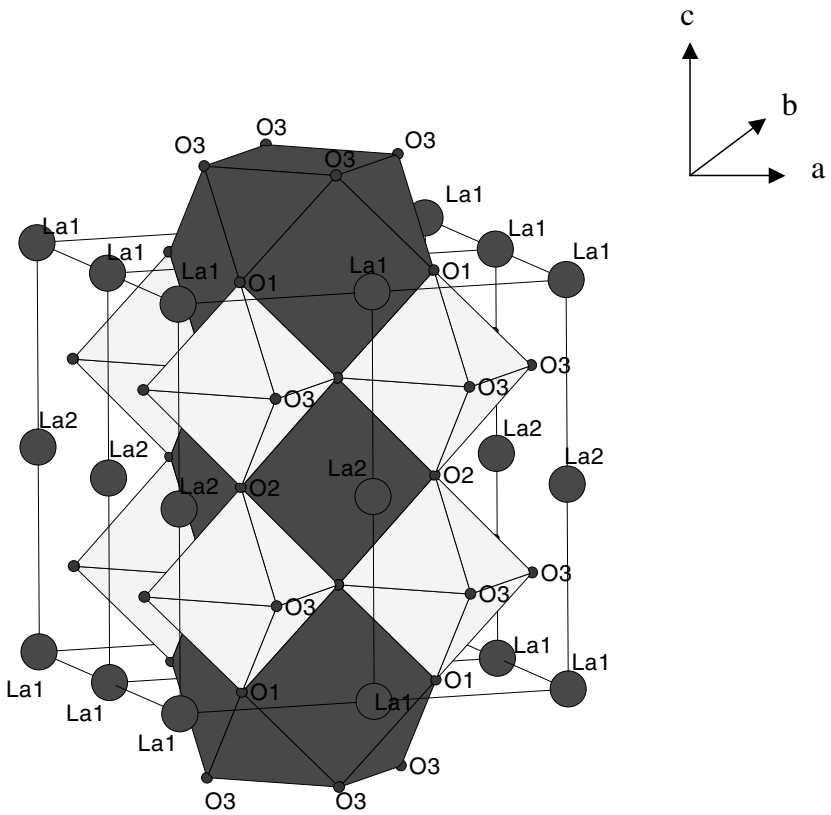

Figure 1. Crystal structure of $(La_{2/3-x}Li_{3x}\square_{1/3-2x})TiO_3$. La1 = La^{3+}, Li^+ or vacancies at position (0, 0, 0); La2 = La^{3+}, Li^+ or vacancies in position (0, 0, 1/2). The unit cell is also shown.

(a further paper will discuss the theoretical aspect). To this end, we chose to perform ^{7}Li NMR experiments on the compound $(Li_{3x}La_{2/3-x}\square_{1/3-2x})TiO_3$ with $x = 0.11$ (known as type B). This particular composition lies in the middle of the solid-solution domain and therefore the presence of impurities that could perhaps be found in compounds lying at the edges of the solid-solution domain is minimized. Experiments on ^{6}Li were also performed in order to discern what interaction governs the relaxation.

2. Experiment

2.1. Preparation of the solid-solution compounds

Samples of different compositions x (known as type A) were prepared as previously described [15]. A sample of type B ($x = 0.11$) was prepared by conventional solid-state reactions from stoichiometric amounts of ultrapure TiO_2 (99.999%), Li_2CO_3 (99.97%) from Aldrich and freshly dehydrated La_2O_3 (99.999%) from Rhone–Poulenc. The starting materials were mixed and pressed into pellets (diameter: 10 mm; thickness ≈2 mm; $P = 250$ MPa). They were first heated at 850 °C for 4 h in a Pt crucible and then heated up to 1050 °C for 12 h. After grinding and pressing, the pellets were heated twice for 10 h at 1100 and 1150 °C. The heating sweep rate was 5 °C min^{-1}. Natural cooling in the furnace followed the heating treatments.

2.2. NMR measurements

The relaxation times T_1, $T_{1\rho}$ and T_2 were measured versus temperature. The experimental set-ups were described in [15–17]. The Larmor frequencies were $\nu_0 = 116$ MHz for ^{7}Li and $\nu_0 = 44$ MHz for ^{6}Li.

Measurements of the longitudinal relaxation times T_1 were performed on ^{7}Li in the temperature range 150–900 K by using both an inversion–recovery sequence (π–τ–$\pi/2$ acquisition) and a saturation pulse sequence. The amplitude of the radio-frequency field was $\nu_1 = 62.5$ kHz for ^{7}Li and $\nu_1 = 15.6$ kHz for ^{6}Li. This corresponds to a non-selective excitation. The two methods lead to the same results. T_1-experiments were performed on ^{6}Li in the temperature range 200–410 K. To improve the signal-to-noise ratio either 64 or 128 transients were accumulated for ^{7}Li and 4K for ^{6}Li. To determine T_1 at each temperature, the experimental magnetization was fitted to the exponential function

$$M(\tau) = M_0\left[1 - 2\alpha \exp\left(-\frac{\tau}{T_1}\right)\right] \tag{1}$$

where the spin–lattice relaxation time T_1, the thermal equilibrium magnetization M_0 and α are considered as free parameters in a least-squares fitting procedure. T_1 was determined by using either the peak area or the peak intensity. The α-parameter, which is not a critical one, was found to be around 0.5 when using the saturation method and around 1 for the inversion–recovery method.

The longitudinal relaxation times in the rotating frame, $T_{1\rho}$, were obtained by using the classic pulse sequence ($\pi/2$–(spin lock) τ acquisition), with a lock radio-frequency field $\nu_1 = 62.5$ kHz for ^{7}Li and $\nu_1 = 15.6$ kHz for ^{6}Li. $T_{1\rho}$-measurements were not performed above 410 K because the high-temperature probe is unable to withstand the power during the locking pulse. To account for the experimental magnetization curve, two spin–lattice relaxation times in the rotating frame were needed and the following relationship was used to determine the $T_{1\rho}$-values:

$$M_{1\perp}(\tau) = M_0\left[a_1 \exp\left(-\frac{\tau}{T_{1\rho}^{\mathrm{S}}}\right) + b_1 \exp\left(-\frac{\tau}{T_{1\rho}^{\mathrm{F}}}\right)\right]. \tag{2}$$

$T_{1\rho}^{\mathrm{S}}$ refers to a slow relaxation process and $T_{1\rho}^{\mathrm{F}}$ to a fast one.

Transverse relaxation times T_2 were obtained with the Carr–Purcell–Meiboom–Gill sequence between 150 and 900 K. As for $T_{1\rho}$, to account for the experimental transverse magnetization two exponential functions were necessary and the following relationship was used to determine the T_2-values:

$$M_{\perp}(\tau) = M_0\left[a_2 \exp\left(-\frac{\tau}{T_2^{\mathrm{S}}}\right) + b_2 \exp\left(-\frac{\tau}{T_2^{\mathrm{F}}}\right)\right]. \tag{3}$$

T_2^{S} refers to a slow relaxation process and T_2^{F} to a fast one.

WINFIT extended software was used to fit the spectra and obtain the peak linewidths, the peak positions (in Hz or ppm), the ratio of each contribution and the quadrupolar splitting [20].

3. Results

3.1. NMR spectra

In figure 2(a), the ^{7}Li ($I = 3/2$) quadrupolar nucleus spectra for samples of type A of different x-values (which corresponds to different conductivity, as described in [15]) are shown. It can be seen that the static ^{7}Li spectra are very sensitive to the conductivity value [15]. At RT,

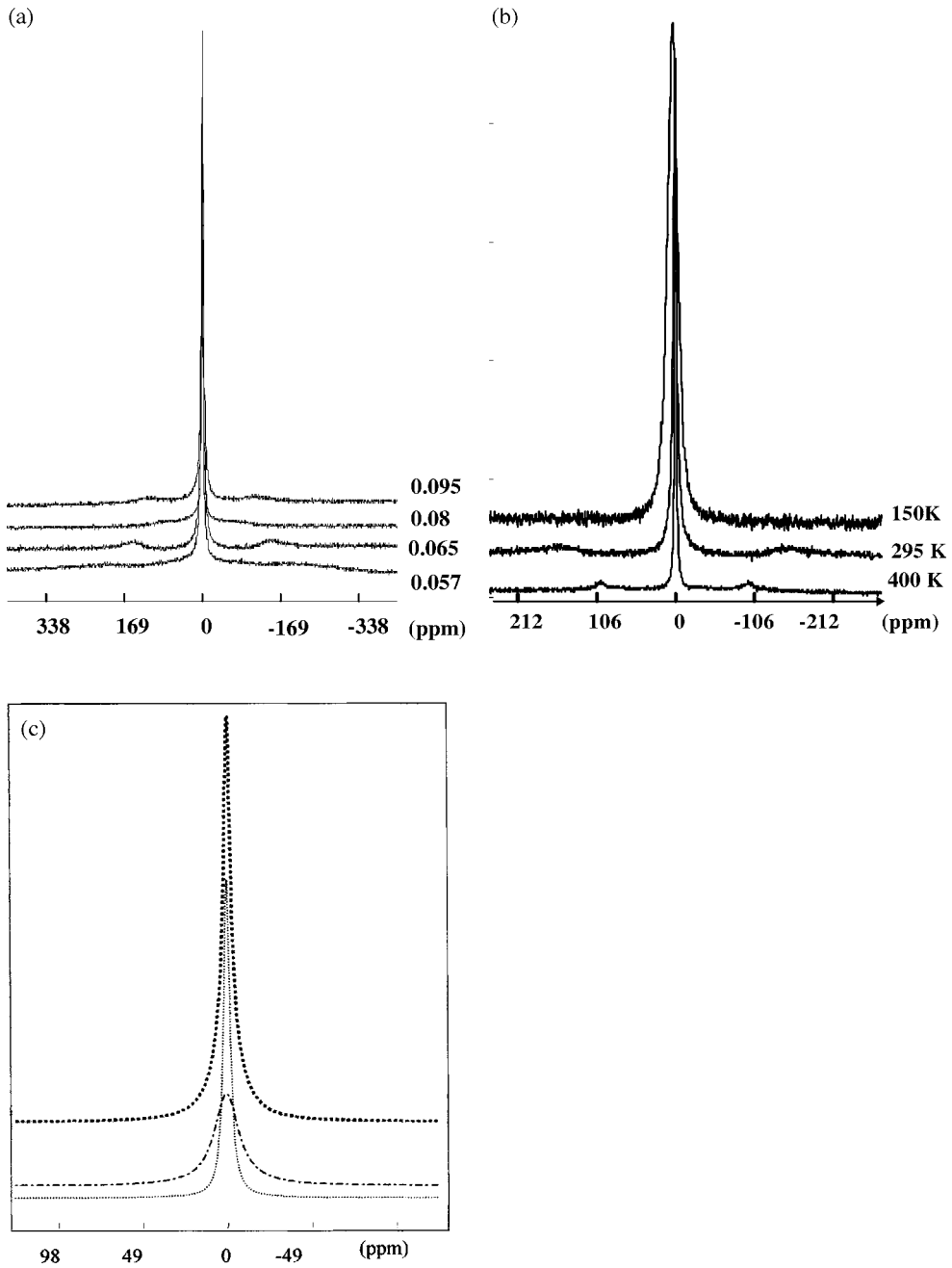

Figure 2. Typical RT static ^7Li NMR spectra recorded at 116 MHz. (a) The behaviour of the satellite transitions with the composition parameter x. (b) The behaviour of the satellite transition with temperature for $x = 0.08$. (c) The spectrum for the type-B sample ($x = 0.11$), synthesized with ultrapure TiO_2. The results presented in this paper correspond to this sample. Two Lorentzian lines (dashed curves) are used to account for the experimental line. The calculated (dotted curve) and experimental (full curve) spectra are exactly superposed.

on samples where the ($\pm 1/2 \leftrightarrow \pm 3/2$) satellite transitions are observed, splitting follows the dc conductivity and is minimum when the dc conductivity is maximum ($0.083 \leqslant x \leqslant 0.09$). One question arises: is this static quadrupolar interaction sensitive to the ionic mobility? If the answer is yes, this means that we observe a motional-averaged quadrupolar splitting and that the Li^+ ions hop into sites with different field gradients. Otherwise, the Li^+ ions hop into sites with the same electric field gradient, leading to apparent static quadrupolar splitting. In any case, this assumption means that the position of the Li^+ ions is never fixed, in contrast to other results [21, 22]. On the other hand, if the answer is no, this means that only the residual quadrupolar splitting is static and that the electric field gradient at the Li^+ site varies with the composition x and then the site distortion also changes. Nevertheless, no conclusion on the site position can be drawn, and we must bear in mind that the La crystallographic site (centre of the A-cage) where the Li^+ ion should be does not give valence one (BVS = 0.2 [5]).

Figure 2(b) shows the temperature behaviour of the ($\pm 1/2 \leftrightarrow \pm 3/2$) satellite transitions for the $x = 0.08$ type-A sample ($\sigma = 4 \times 10^{-4}$ S cm^{-1} at RT). In this diagram we see that the satellite splitting behaves in the same way with temperature as with conductivity: the smaller the splitting, the higher the dc conductivity. Thus, we must choose the Li^+-ion motion hypothesis and the Li^+ position cannot be defined. The satellites also become clearer as temperature increases (above 400 K). This can be explained according to the following hypothesis. When temperature increases, the motion averages the interactions seen by the Li^+ ions: we observe an average quadrupolar splitting value and not an instantaneous one. Furthermore, this motion also has some effect on the individual linewidths. This narrowing arises at the individual lines in the powdered sample, but is clearer for the satellite transitions.

Some authors [22] conclude that the structure of LLTO becomes cubic upon quenching, because their experimental ^{7}Li NMR static spectra do not display any satellites. In our opinion much care must be taken in the interpretation of the absence of the satellite transitions because these satellite transitions can be very broad but nevertheless present in the spectrum. The right way to proceed would be for the authors to check whether the central transition remains unbroadened after the quenching process.

Figure 2(c) shows the ^{7}Li NMR spectrum recorded at 295 K for the type-B sample. It corresponds to the composition $x = 0.11$ with a dc conductivity of 5×10^{-4} S cm^{-1} at RT. Because the quadrupolar satellite transition splitting is very weak for this sample at this temperature, no singularities corresponding to the satellite transitions are clearly observed. Nevertheless, we need two lines to account for the shape of the spectrum.

To avoid any ambiguity which may arise from the satellite transitions in quadrupolar nuclei during excitation, we present in this paper the results obtained on a type-B sample with $x = 0.11$ for which the quadrupolar satellite transition splitting is very weak at RT (figure 2(c)). Nevertheless, most of the results (T_1, T_2, $T_{1\rho}$) are common to all the samples, either A or B types, with a variable conductivity and for samples with or without observed quadrupolar splitting [15–18, 23].

In this sample, above 200 K two Lorentzian lines account for the ^{7}Li NMR spectrum with variable proportions. Figure 3 shows the linewidths (a), the line positions (b), the percentages of the two line contributions (c) and a MAS spectrum obtained at 15.5 kHz (d). The linewidths (figure 3(a)) remain relatively narrow even at low temperature (down to 210 K), and the two lines are clearly discerned. Below 200 K only one line is clearly detected; the broader line is difficult to see but nevertheless it is present in the spectrum, and the results become less accurate. We also observe a particular behaviour of the broader line when temperature decreases: the linewidth begins to increase down to 250 K and then it decreases slightly between 250 and 220 K, and it increases again down to 200 K. In figure 3(b) variations with temperature of the relative contributions from the two lines are also visible. In

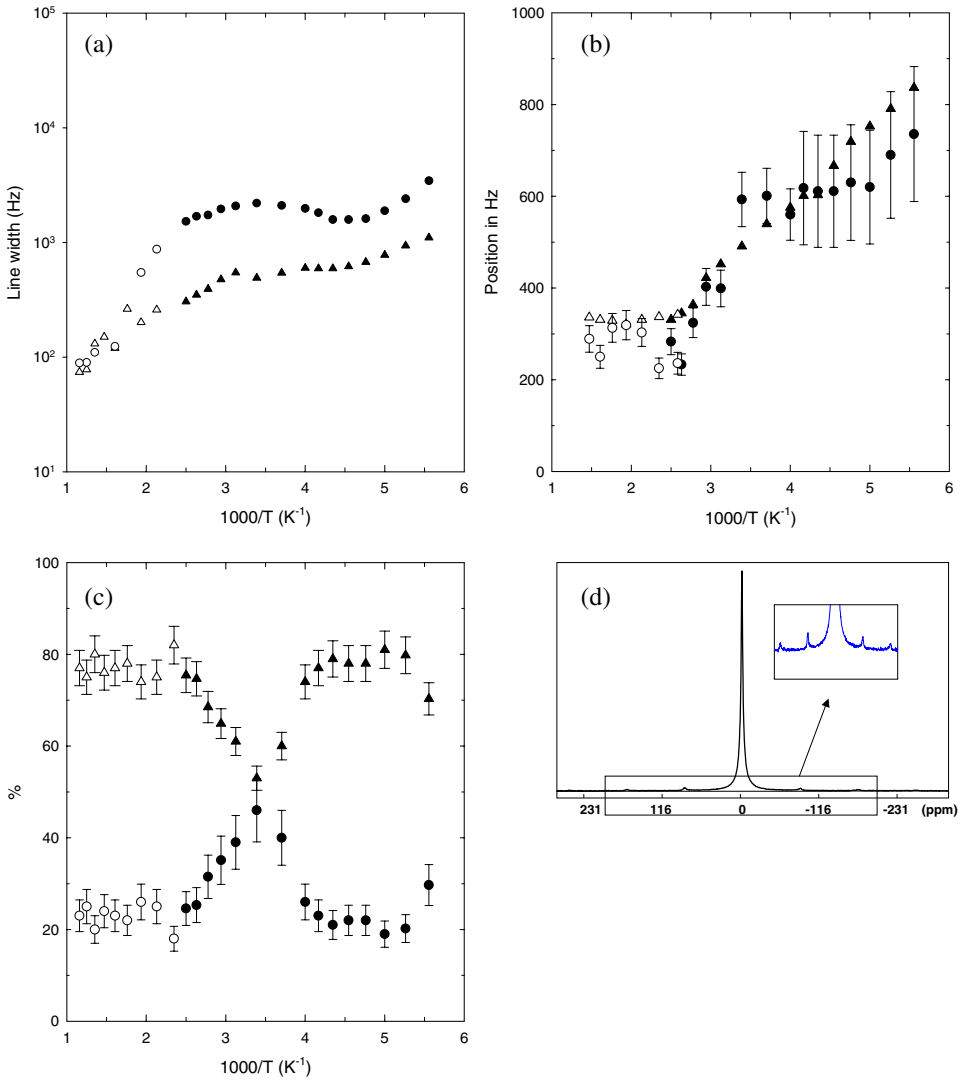

Figure 3. Temperature dependence of the static ^{7}Li NMR spectra parameters (●, ▲ = 150–410 K and ○, △ = RT to 1000 K); circles and triangles stand for the narrow and broad lines respectively. (a) Linewidths. (b) Line positions. The experimental errors are larger at low temperature owing to the line broadening. (c) Percentages of the two line contributions. (d) The magic angle spinning spectrum obtained at 10 kHz: spinning sidebands due to the satellite transitions spread over more than 50 kHz (inset).

(This figure is in colour only in the electronic version)

figure 3(c) we see that the two lines collapse at high temperatures while they are separated at low temperatures.

3.2. Longitudinal relaxation time T_1-results

The spin–lattice relaxation times T_1 for ^{7}Li are presented in figure 4 as a function of the inverse of temperature, in the temperature range 150–900 K. The main features exhibited by this relaxation time T_1 are:

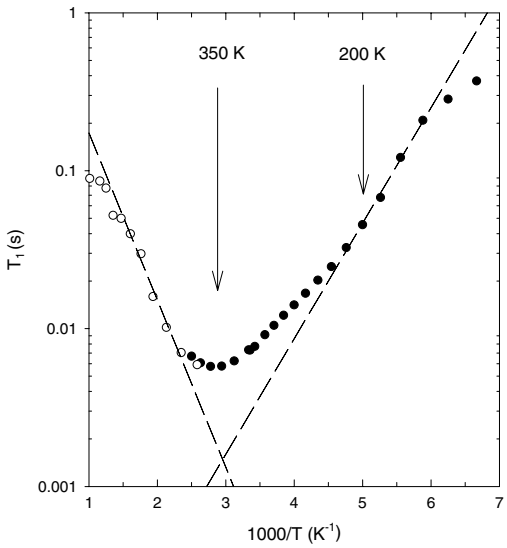

Figure 4. A logarithmic plot of T_1 for ^{7}Li ($\nu_0 = 116$ MHz) as a function of the inverse of temperature for $(La_{2/3-x}Li_{3x}\square_{1/3-2x})TiO_3$, $x = 0.11$ (● = 150–410 K and ○ = RT to 1000 K). The dashed curves represent linear regressions of the data at low ($E_a = 0.14$ eV) and high temperatures ($E_a = 0.20$ eV).

(i) A mono-exponential magnetization curve; i.e. only one T_1 is observed whatever the method used. A wide range of values of τ have been used from 10 μs to 1s.
(ii) The presence of a minimum around 350 K.
(iii) A particular behaviour around 200 K.
(iv) A strong asymmetry around the minimum.

It must be noted that all these peculiarities are general features of T_1 in LLTO whether or not the satellite transitions are observed [15–18].

3.3. Relaxation time in the rotating frame $T_{1\rho}$-results

The relaxation times in the rotating frame, $T_{1\rho}$, as a function of the inverse of temperature are shown in figure 5 for ^{7}Li. Above 300 K only one value of $T_{1\rho}$ was observed, while two values were measured below this temperature to account for the experimental magnetization curve. Each curve shows a minimum: for $T_{1\rho}^S$ it appears around 280 K and for $T_{1\rho}^F$ at 250 K. Each of the two curves also shows a peculiarity around 200 K.

3.4. Transverse relaxation time T_2-results

The transverse relaxation times T_2 as a function of the inverse temperature are shown in figure 6. To account for the experimental transverse magnetization, two transverse relaxation times, T_2^S and T_2^F, were necessary below 370 K. Above 370 K, the two relaxation times could not be distinguished from one another and only one value was obtained. The two relaxation times, T_2^S and T_2^F, are thermally activated. Above 400 K, an activation energy of 0.20 eV was determined for the single relaxation time observed. Below 250 K, T_2^F is thermally activated with an activation energy of 0.15 eV and below 200 K, T_2^S is thermally activated with a low activation energy of 0.06 eV. Additionally, T_2^S and T_2^F behave in an interesting way in the

same temperature range as T_1 and $T_{1\rho}$, as shown in figure 6: T_2^F displays an inflection point between 250 and 285 K weakly shifted from the T_1-minimum (i.e. 350 K) and T_2^S displays a near-constant value between 200 and 280 K.

4. Discussion

4.1. NMR spectra

Whatever the temperature, the ratio of the two contributions is never in the (4:6) ratio expected for central and satellite transitions in an $I = 3/2$ spin system. Such a splitting, that is valid for a static system, exists only in a restricted temperature range in our case. We cannot conclude from this result that we do not observe central and satellite transitions.

Indeed, on the one hand, we must be careful when we use the percentage of the different contributions because when temperature decreases and we reach the slow-regime limit or low-temperature range, the satellite transitions broaden more rapidly than the central one and progressively disappear, thus introducing a temperature variation in the contributions to the spectrum. On the other hand, in the fast regime the proportions would remain constant with temperature, particularly above RT where the two lines are relatively narrow and distinct. However, in the very fast regime the central and the satellite transitions behave in the same way. Thus, between the two extreme regimes the different contributions vary with temperature. So this is what we observe in figure 3(c), and we could conclude that we indeed observe the central and satellite transitions and that consequently only one type of lithium is present.

To overcome these difficulties and to choose between these two hypotheses, we recorded spectra at another frequency. Theoretically, the splitting of the satellite does not depend on the Larmor frequency. At RT, the spectrum recorded on an Avance 400 spectrometer, where the ^7Li nucleus resonates at 155 MHz, reveals two lines with the linewidths of 759 and 4129 Hz respectively. The spectrum recorded on an Avance 300 with the ^7Li nuclear resonance frequency at 116 MHz also reveals two lines with linewidths of 641 and 3475 Hz respectively. The respective linewidth values follow the ratio of the Zeeman frequencies. So the two lines observed in the NMR spectrum cannot be ascribed to quadrupolar effects, but correspond to two Li^+ sites, and the broadening arises from disorder and/or some inhomogeneity.

Figure 3(d) presents a MAS experiment performed at RT with a spinning frequency of $\nu_R = 10$ kHz. The two intense lines previously observed in static experiments remain in the same position and their linewidths narrow (270 Hz instead of 659 Hz for the narrow line and 916 Hz instead of 3475 Hz for the other line); the ratio is 55/44. On the other hand, several spinning sidebands spread over 120 kHz when the spin-rotation frequency is $\nu_R = 25$ kHz, which shows anisotropic effects. The spinning sideband positions (at a multiple of ν_R from their isotropic line) do not correspond exactly to replicas of the intense line. Thus, they must be ascribed to satellite transitions. Each of them is the superimposition of two lines wider apart than the central transitions. This means that the intense line corresponds to two Li^+ sites and that the linewidths are sensitive to an anisotropic interaction.

Finally, figure 3(b) shows a variation of the line positions with temperature. The lines shift in the same way and this may be ascribed either to the temperature evolution of the lattice parameters or to the dynamical shift due to the fluctuation amplitudes that slow down when temperature decreases. According to this hypothesis the lines would shift toward high frequency when temperature decreased, and this is what we observed for our sample.

Thus two Li^+ sites are observed. Nevertheless, we cannot attribute these contributions to Li^+ in the 1a (La^{3+}-rich) or 1b (La^{3+}-poor) layer except in the low-temperature region where the Li^+ ions do not hop between planes (see below).

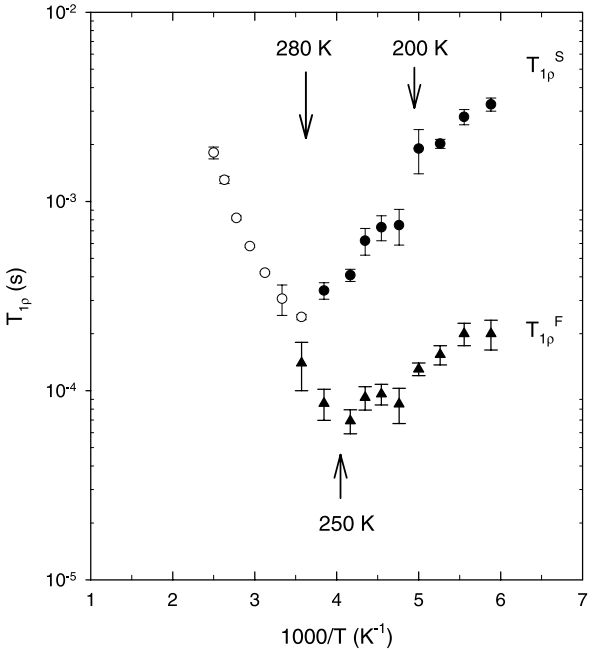

Figure 5. A logarithmic plot of $T_{1\rho}$ for ^{7}Li ($\nu_1 = 62.5$ kHz) as a function of the inverse of temperature for $(La_{2/3-x}Li_{3x}\square_{1/3-2x})TiO_3$, $x = 0.11$ (● and ▲ = 150–410 K and ○ = RT to 1000 K).

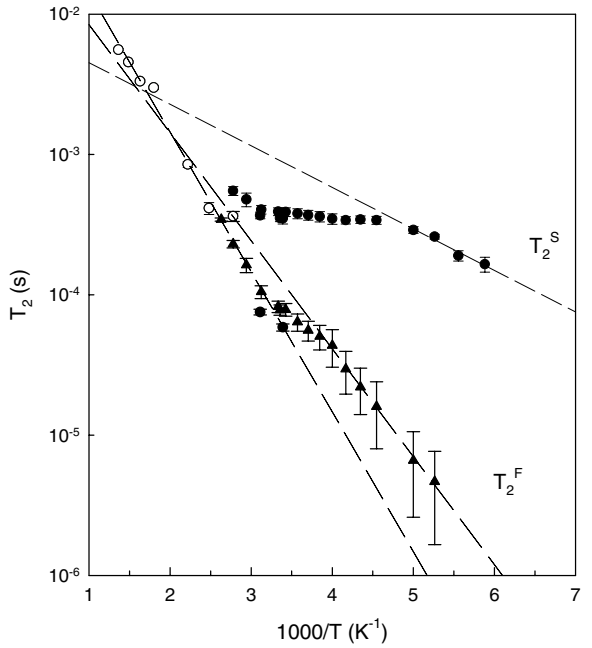

Figure 6. A logarithmic plot of T_2 for ^{7}Li as a function of the inverse of temperature. A plateau for T_2^{S} is observed in the temperature range in which T_1 and $T_{1\rho}$ also exhibit a particular behaviour. The dashed curves are linear regressions of the experimental data with activation energy $E_a = 0.20$ eV in the fast regime and 0.15 and 0.06 eV in the slow regime for T_2^{F} and T_2^{S} respectively. Error bars increase as temperature decreases owing to the small T_2^{F}-contribution to the FID.

One point remains to be clarified: why are the satellites smoothed when the central transition is not so broad and why, in type-B samples, are the satellites clearer at high temperatures than at low ones. Three reasons may be put forward: firstly, the disorder which gives rise to a quadrupolar parameter distribution acts at the first order of perturbation on satellites and at the second order on the central line; secondly, even interactions (quadrupolar or dipolar between like spins) do not bring about any adiabatic contribution to the central transition [24]; the third reason is dynamic: when dipolar broadening is larger than the quadrupolar splitting, ν_Q^2/ν_0, ν_Q being the quadrupolar parameter, the line disappears into the noise; at high temperatures the motion narrows the dipolar interaction and the lines merge.

To conclude this section, we must point out the special behaviour of the broader line: its width begins to increase when temperature decreases, then between 280 K and 210 K it decreases. Below this temperature the two linewidths increase as expected in the slow regime. Special behaviour is also observed in the T_2-parameters in the same temperature range and will be analysed below.

4.2. Relaxation times

From a general point of view, the relaxation time varies according to the type of the interaction involved in the mechanism of relaxation, the amplitude of the fluctuations and the spectral density. Therefore, a relaxation time T_α (α standing for 1, 2 or 1ρ) can be expressed by the following relationship:

$$\frac{1}{T_\alpha} = |C_\lambda|^2 \left\langle \delta_\lambda^2 \right\rangle F\left(J\left(\omega_0, \omega_\alpha\right)\right) \tag{4}$$

where C_λ is the parameter characterizing the interaction (the quadrupolar moment Q for a quadrupolar interaction, the product of the gyromagnetic ratio of the two nuclear spins for a dipolar interaction), $\langle \delta_\lambda^2 \rangle$ is the amplitude of the fluctuation (the electric field gradient in the quadrupolar case, the $\vec{r}$-vector between two magnetic moments in the dipolar case and/or θ, the angle between $\vec{r}$ and the static magnetic field direction) and $F\left(J\left(\omega_\alpha\right)\right)$ is a function of the fluctuation spectral density and ω_0 is the Larmor angular frequency. ω_α is the characteristic angular frequency for the relaxation time T_α, i.e. $\omega_\alpha = 0$ for T_2; $\omega_\alpha = \omega_1 = \gamma B_1$ is that for $T_{1\rho}$; $\omega_\alpha = \omega_0$ is that for T_1; $\omega_\alpha = (\omega_I - \omega_S)$ for cross-relaxation between spins I and S.

4.3. Longitudinal relaxation time T_1

As ^{7}Li is a quadrupolar nucleus, we expect to observe two spin–lattice relaxation times T_1 for each Li site, one for the central line and one for the satellites (see [24–28] and references therein). Surprisingly, the experiment evidences only one value of T_1 common to all the transitions. However, it must be mentioned that if the spin–spin relaxation time is fast [29] or if the relaxation mechanism is not a quadrupolar one, only one T_1-value is observed. On the other hand, if the spacing between lines becomes comparable with the dipolar linewidth, a common temperature of the spin system is established by rapid spin–spin interactions leading to a single spin–lattice relaxation time for the two sites [30]. Moreover, the plot of T_1 versus $1000/T$, shown in figure 4, clearly displays a strong asymmetric shape and a peculiar behaviour around 200 K. This peculiar behaviour is also present in the T_2 and $T_{1\rho}$ versus $1000/T$ plots at the same temperature, as we shall see later.

The asymmetry between slow and fast regimes mirrors a ratio very close to 1.5 in the activation energy. This asymmetry may be caused by an ionic diffusion occurring in low dimension, i.e. 1D or 2D, as described by Richards [29], by either a distribution of the activation energy [16], by a distribution of the correlation time or by the cation hopping dynamics itself.

Richards' assumption, i.e. an ionic motion confined to one or two dimensions (1D or 2D), is commonly encountered in superionic conductors because of structural features. According to Richards [29], a dimensionality effect would lead either to a steeper slope at low temperatures than at high temperatures for a 1D or 2D motion or to a symmetric curve for a 3D motion. Figure 4 clearly shows that the slope of the $\log(T_1)$ versus $1000/T$ curve is greater at high temperatures than at low temperatures. This behaviour has been observed for all the compounds studied whatever the composition x [15–17]. It is, then, a characteristic of the solid-solution compounds. This experimental feature does not support a low-dimensionality conductivity effect and Richards' assumption must be ruled out.

In a previous paper we used a distribution of activation energy to model T_1- and σ_{dc}-data [16]. However, by measuring the different relaxation times, i.e. T_1, $T_{1\rho}$ and T_2, we show herein that Li^+ ions exhibit different motions. It becomes clear that T_1 and σ_{dc} do not probe the same ionic motion and that our assumption of distribution of activation energy must be reconsidered. It is worth noting that a distribution of activation energy and a distribution of correlation times, arising from a superimposition of motions, lead to the same mathematical relationship and cannot be distinguished with this method.

Finally, an ion hopping dynamic effect can be postulated to explain this asymmetric behaviour. For example, a change in dimensionality or in the amplitude of the fluctuations, which governs the relaxation, could appear when temperature varies. This assumption agrees with the particular activation energy ratio of 1.5 between the slow and fast regime that was determined. This would indicate a change in the motion dimensionality from a 2D motion at low temperatures to a 3D motion above RT [31]. As temperature increases, new pathways become available for the Li^+-ion motion. Therefore the modification of the environment of the Li^+ ion during its motion through the oxide structure modifies the interactions responsible for its relaxation.

In order to cast light on the nature of the interactions involved in the relaxation mechanism, experiments on the ^6Li nucleus, whose frequency resonance is 44 MHz, were performed. This isotope is not very abundant and its spin is not very high ($I = 1$) compared to the other nuclei present in this material. The ^6Li nucleus has a quadrupolar moment which is 60 times lower than that of the ^7Li one (i.e. $Q(^6Li) = -8 \times 10^{-32}$ m^2, $Q(^7Li) = -4.5 \times 10^{-30}$ m^2), so if the relaxation mechanism originates from quadrupolar mechanism, it would be 3600 times longer for ^6Li nuclei than for ^7Li ones. Furthermore, because this is the same ion, it experiences the same motion as ^7Li. The experimental T_1-data are shown in figure 7 as a function of inverse temperature. It can be observed that T_1 for ^6Li (i.e. 15 ms) is of the same order of magnitude as for ^7Li (i.e. 5.8 ms). In addition, the ratio $T_1(^6Li)/T_1(^7Li) \cong 2.6$ is in the range of the squared ratio between the gyromagnetic constants of the two nuclei ($\cong 7$); the small difference may arise from the contributions of the spectral density at the different frequency measurements. These two results clearly show that the Li relaxation mechanism is not dominated by quadrupolar interaction, as previously suggested by Paris *et al* [23]. Furthermore, the absence of an ESR signal down to 120 K in our materials, and a result for T_1^*T which varies with temperature, rule out a possible dipolar interaction between Li nuclei and some electrons which could be present in the conduction band, as shown by Korringa [32]. Because of its small quadrupolar parameter and low gyromagnetic ratio, the linewidth and line position of this isotope are less sensitive than the ^7Li ones and cannot give complementary information.

Thus it follows that dipolar nuclear interaction or chemical shift must be responsible for the Li relaxation. However, for Li nuclei, the chemical shift remains very low and therefore only dipolar interaction should be considered in the relaxation process. This result is very important and is at variance with what has been previously suggested for the relaxation process in these compounds [23]. The dipolar nature of the interaction responsible for the Li relaxation does

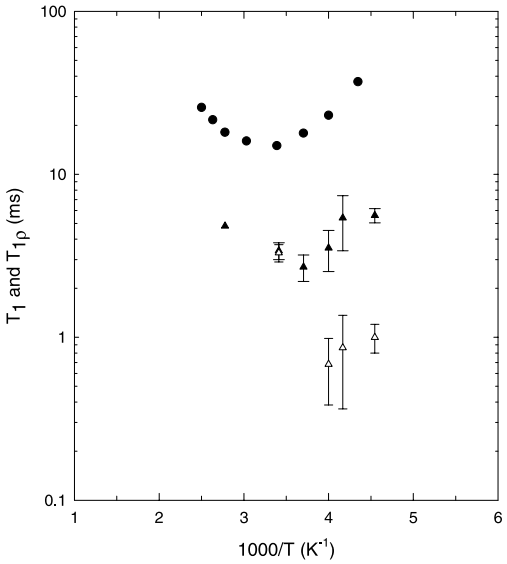

Figure 7. Logarithmic plots of T_1 (●) and $T_{1\rho}$ (▲, △) for ^{6}Li ($\nu_1 = 15.5$ kHz) as a function of the inverse of temperature for $(La_{2/3-x}Li_{3x}\square_{1/3-2x})TiO_3$, $x = 0.11$.

explain the experimental fact that only one T_1 is observed although the nucleus is a quadrupolar one. Furthermore, the two Li^+ ions experience motion in the same way. Both the asymmetric shape of the T_1-curve shown in figure 4 and the peculiar behaviour around 220 K can then be ascribed to change in these dipolar interactions as temperature varies and therefore to change in the hopping mechanism of the Li^+ ions.

T_1-experiments performed on ^{7}Li and ^{6}Li indicate that a motion with a characteristic correlation time $\tau_c = 1/\nu_c$, ν_c being the characteristic frequency, and obeying the relationship $\omega_0\tau_C \approx 1$ at the minimum, is probed by the nuclei. The correlation time of the Li motion is thermally activated and exhibits the relationship

$$\tau_c = \tau_0 \exp\left(\frac{E_a}{k_B T}\right) \tag{5}$$

where E_a is the activation energy of the Li motion and k_B is the Boltzmann constant. According to the relationship $\omega_0\tau_C \approx 1$ at the minimum, the correlation time of this motion is around 10^{-9} s at 350 K. The ratio of the minimum correlation time for ^{7}Li and ^{6}Li follows the ratio of the corresponding resonant angular frequency of the two nuclei (i.e. 116 MHz for ^{7}Li and 44 MHz for ^{6}Li). The minimum of T_1 for ^{6}Li arises at a lower temperature (i.e. 290 K) than for ^{7}Li (i.e. 350 K) and the activation energy of the Li motion probed at the Larmor frequency and calculated from the relationship (5) is found to be 0.14 eV. It is in very close agreement with the activation energy of the Li motion probed by the spin–lattice relaxation time T_1.

4.4. Longitudinal relaxation time in the rotating frame $T_{1\rho}$

The main feature appearing in figure 5 (^{7}Li) is the presence of two values for $T_{1\rho}$ at low temperatures and only one value above 300 K. Furthermore, a peculiar behaviour is also observed in the plot around 200 K as for the T_1-curve. The presence of two values for $T_{1\rho}$ cannot be ascribed to the quadrupolar nature of the nucleus because the theoretical contribution of each relaxation time (for the central line and for the satellites) would be constant and equal

to 20% for the slow contribution and 80% for the fast one [24–28]. The contributions of the two relaxation times do not follow these values, and vary with temperature. This result and the above discussion on T_1 definitively rule out this assumption.

Each curve of $T_{1\rho}$ versus $1000/T$ shows a minimum. For the slowest $T_{1\rho}$ ($T_{1\rho}^{S}$) the minimum ($\approx$0.3 ms) appears at 280 K and for the fastest ($T_{1\rho}^{F}$; $\approx$70 μs) it appears around 250 K. The same features are displayed by the $T_{1\rho}$-plots obtained for ^{6}Li (figure 7). Two $T_{1\rho}$-values are observed below 300 K and only one value above this temperature. These values are of the same order of magnitude as for the ^{7}Li nucleus. Each of these $T_{1\rho}$-plots displays a minimum around 280 K. The ratio between the two values, $T_{1\rho}(^6\mathrm{Li})/T_{1\rho}(^7\mathrm{Li}) \cong 7$ for the fastest one and $T_{1\rho}(^6\mathrm{Li})/T_{1\rho}(^7\mathrm{Li}) \cong 8$ for the slowest one, is very close to the squared ratio between the gyromagnetic constants of the two nuclei ($[\gamma(^7\mathrm{Li})/\gamma(^6\mathrm{Li})]^2 \cong 7$) involved in a heteronuclear spin–spin relaxation. The agreement is better than for the T_1-ratio and suggests a particular shape of the spectral density

The minimum for T_1 (116 or 44 MHz) and for $T_{1\rho}$ (62.5 or 15.5 kHz) occurs in the same temperature range: at 350 K for T_1 and at 280 and 250 K for the two $T_{1\rho}$. The three decades between the frequency cannot be explained by the temperature difference observed in the minima of T_1 and $T_{1\rho}$. According to the relationship $\omega_0\tau_C \approx 1$ at the minimum, the correlation time of the motion probed by $T_{1\rho}$ is around 10^{-6} s at 280 K. This result means that T_1 and $T_{1\rho}$ probe two different ionic motions: one fast around 100 MHz at RT and one slow around 70 kHz at 280 K.

4.5. Transverse relaxation time T_2

Figure 6 shows the variations of the transverse relaxation time as a function of inverse of temperature. The experimental transverse magnetization curve versus time reveals the presence of two relaxation times T_2: a slow one known as T_2^S and a fast one known as T_2^F. Below 200 K, T_2^F is more highly activated ($\approx$0.15 eV) than T_2^S ($\approx$0.06 eV). T_2^F shows an inflection point around 350 K as it generally appears near the minimum of T_1. From 200 to 300 K T_2^S exhibits a plateau. This particular behaviour occurs at the same temperature as the T_1- and $T_{1\rho}$-abnormalities (i.e. 200 K). This feature can be ascribed to the same change in the dipolar relaxation mechanism of Li^+ nuclei.

The above results obtained from T_1-, $T_{1\rho}$- and T_2-experiments with the ^{7}Li nucleus prove beyond doubt the presence of two different Li^+ ions with differing environments in the structure of this oxide. This result is confirmed by the existence of two $T_{1\rho}$ with the ^{6}Li nucleus with $S = 1$. Ions of each kind experience two motions, one fast with a correlation time in the region of a nanosecond at 350 K and one slow with a correlation time in the region of a microsecond at 280 K. However, the presence of only one T_1, two $T_{1\rho}$ and two T_2 means that these different ions can be differentiated by means of the slow motion only. This also explains why they can be differentiated in the static spectra.

4.6. Relaxation mechanism and motion of Li^+ nuclei

The above discussion clearly shows that the relaxation mechanisms involved in T_1, T_2 and $T_{1\rho}$ are dipolar. These relaxation times (for a dipolar relaxation mechanism) follow the spin Hamiltonian

$$H = \sum_{i<j} \sum_{q=-2}^{+2} D_{ij}^{(q)} T_{ij}^{(-q)} \tag{6}$$

where the first summation is over the pairs of spins i and jq accounts for the qth component of the irreducible tensor of rank 2 ($\tilde{D}$ or $\tilde{T}$). $D_{ij}^{(q)}$ is the qth component of the dipolar tensor

connecting nuclear spins i and j, $T_{ij}^{(q)}$ is the qth component of the irreducible tensor constructed with spins i and j (magnetic) which can be like or unlike spins. In the relaxation time, correlation functions expressed as

$$\sum_{q,q'=-2}^{+2}\left\{\sum_{(i,j)}\sum_{(i',j')}\left\langle D_{ij}^{(q)}(0)D_{i'j'}^{(-q')}(\tau)\right\rangle\right\} \tag{7}$$

are involved and if we ignore correlation between terms with different q' only summation on q remains. Therefore, the relation (7) splits into a sum of two terms:

$$\sum_{q=-2}^{2}\left\{\sum_{(i,j)}\left\langle D_{ij}^{(q)}(0)D_{ij}^{(-q)}(\tau)\right\rangle+\sum_{(i,j)}\sum_{(i',j')\neq(i,j)}\left\langle D_{ij}^{(q)}(0)D_{i'j'}^{(-q)}(\tau)\right\rangle\right\}. \tag{8}$$

This relationship separates the contribution of individual pairs and the contribution of correlated pairs. The interesting behaviour in T_1 can be viewed as another contribution to T_1 that lowers its value. At the same time, the minimum of T_1 is shifted towards high temperature. Thus, several assumptions can be made to explain the presence of the anomaly in the T_1-, $T_{1\rho}$- and T_2-curves versus $1000/T$.

The first is linked to the presence of a correlated motion. Indeed, at low temperature in the rigid-lattice limit, no correlation exists between ionic motions and therefore just the first term of (8) accounts for this phenomenon. When temperature increases, some correlation between pairs arises and the second term is added as a new contribution to the relaxation time. Therefore $1/T_1$ increases, leading to a sudden decrease in T_1 at this temperature. Because the fluctuation amplitude is included in all the relaxation times, this term is also included and contributes further to $1/T_2$ and $1/T_{1\rho}$. This assumption means that a correlated motion occurs above 200 K and is responsible for a modification of the relaxation mechanism and consequently for a sudden change in the relaxation times as observed.

The second way to explain a decrease in T_1 is by a change in the fluctuation amplitude, $\langle\delta_\lambda^2\rangle$, around 200 K. Considering only the first term in relation (8), if the fluctuation amplitude increases above 200 K, the value of $1/T_1$ increases, leading to a decrease in T_1. A change in the fluctuation amplitude means that the pathways for ionic motion are altered, leading to a change in the relaxation mechanism. Because the q-component bears the motion symmetry, any change in fluctuation can activate a particular q-component of the Hamiltonian (6).

Interaction between unlike spins in the relaxation process, a particular mechanism named cross-relaxation, may also explain this unusual behaviour. So the two spins are subject to two types of spin–lattice relaxation. The first corresponds to the direct relaxation of either the I-spin (observed spin) or S-spin to the lattice and the second corresponds to both the direct and indirect relaxation via the cross-relaxation. At low temperature, the cross-relaxation largely dominates the process because the cut-off of the spectral density corresponds to the characteristic frequency $|\omega_I-\omega_S|$. This contribution enhances $1/T_1$ by a factor of $\omega_I/(|\omega_I-\omega_S|)$ and thus decreases T_1 [24].

Of all these hypotheses, it is a change in the motion which accounts for all the behaviours of the T_1-, T_2-, $T_{1\rho}$-parameters as well as for the dc and ac conductivity anomalies observed in the same temperature range [12].

As described above, just dipolar fluctuations are responsible for the relaxation mechanism. Because the relaxation mechanism arises from fluctuations $\langle\delta_\alpha^2\rangle$ of the coupling between the nuclear spin and its neighbourhood and because these fluctuations result from Li^+-ion hops between sites with different environments, the Li^+-ion hops bring the ions into different sites with either exactly the same quadrupolar Hamiltonian or fluctuations of quadrupolar interactions smaller than the dipolar ones. Because quadrupolar interactions are more confined than

dipolar ones, the longitudinal relaxation experiences long-distance interactions. According to the crystallographic structure shown in figure 1, the Li^+ ions are located near the A-site of the perovskite structure surrounded by 12 oxygen ions which are the nearest neighbours. Ti^{4+} ions (there are a few ^{47}Ti, $I = 5/2$ and ^{49}Ti, $I = 7/2$) are their next-nearest neighbours. There is only a weak dipolar interaction with these ions, and possibly a very weak quadrupolar interaction. Therefore, the dipolar coupling which governs the longitudinal relaxation must involve the second-next-nearest neighbours of ^7Li, namely the ions present in the six surrounding A-sites of this Li^+ ion (i.e. Li^+, La^{3+} or vacancy). This coupling may then be either homonuclear (i.e. between ^7Li nuclei) or heteronuclear (i.e. between ^7Li and ^{139}La); these two nuclei are sufficiently abundant to influence the dipolar relaxation. During its hop from one A-site to the next vacant one, the Li^+ ion leaves its A-site surrounded by given second-next-nearest neighbours to occupy a new A-site with a different environment, leading to a variation in its dipolar fluctuations much greater than that in its quadrupolar fluctuations.

The presence of two types of Li^+ ion is linked to the uneven occurrence of La^{3+} ions among the 1a and 1b sites of the structure. As a result, some Li^+ ions are surrounded by many La^{3+} ions and other Li^+ ions are surrounded by many vacancies, leading to different environments for the Li^+. The two motions of these Li^+ ions can also be explained by considering the structure. Because it is small compared to the size of the A-cage, the Li^+ ion is located not in the centre of the A-cage but inside a funnel-shaped volume [5]. Therefore, it can move rapidly inside the A-cage. This motion is detected via the longitudinal relaxation time T_1 at the Larmor frequency. Its correlation time is in the region of 10^{-9} s at 350 K with an activation energy of 0.13 eV at this temperature. Secondly, the Li^+ hops from one A-cage to the next occupied by a vacancy. This motion is slower than the first and is detected via both the relaxation time in the rotating frame, $T_{1\rho}$ at 62.5 kHz, and via the transverse relaxation time T_2. Its correlation time is in the region of 10^{-6} s at 280 K with an activation energy of 0.21 eV at this temperature. To perform such a hop, the ion has to cross a bottleneck made of four oxygen ions as shown in figure 1. These bottlenecks differ depending on both the crystallographic direction and the type of the A-cage. As described in [12], the A-cages belonging to the La^{3+}-rich layer (1a) are smaller than the A-cages belonging to the La^{3+}-poor layer (2a). This leads to the presence of smaller bottlenecks in this (1a) layer and consequently it becomes difficult for the Li^+ ions to move. On the other hand, the Li^+ ions belonging to the (2a) layer move more easily. However, their motion depends on the direction. In the $\vec{a}$- and $\vec{b}$-directions (figure 1) the bottlenecks are all identical (lozenges), and they are bigger than in the $\vec{c}$-direction (square). The size of these bottlenecks changes as temperature increases because of the thermal agitation of the oxygen ions. At low temperature ($T < 200$ K) only the bottlenecks in the $\vec{a}$- and $\vec{b}$-directions are large enough to allow Li^+ hops, leading to a 2D motion. When temperature increases above 200 K the oxygen vibrations open the bottlenecks along the $\vec{c}$-direction, thus allowing Li^+ hops along the third direction.

5. Conclusions

In this paper we have given NMR experiment results concerning the Li^+ dynamics of the $Li_{3x}La_{2/3-x}\square_{1/3-2x}TiO_3$ fast-ionic conductors in order to give an insight into the ionic motion mechanism. We analyse general features of the spectra and of the relaxation times T_1, T_2 and $T_{1\rho}$ of the ^7Li nucleus and T_1 and $T_{1\rho}$ of ^6Li versus temperature. The relaxation of the ^7Li nucleus is characterized by one T_1, two T_2 and two $T_{1\rho}$. The same observations also hold for ^6Li T_1- and $T_{1\rho}$-parameters.

The T_1-curve displays a minimum at 350 K which allows us to predict a motion with a characteristic frequency $\nu_C = 116$ MHz (^7Li resonance frequency) at 350 K and 44 MHz (^6Li resonance frequency) at 290 K and a particular behaviour around 200 K.

The two $T_{1\rho}$ also show a minimum and also display an anomaly at the same temperature as that of T_1. This particular behaviour is more pronounced for the slow $T_{1\rho}$. This new motion with characteristic frequency equal to 62.5 kHz does not correspond to the previous one detected with the T_1-minimum (the difference of three decades in frequency cannot be compensated by the 70 K temperature difference). These two motions are attributed to a rapid motion of Li^+ inside the A-cage formed by twelve oxygen ions and a slow motion between the cages through the bottleneck formed by four oxygen ions.

The study of the ^{6}Li T_1- and $T_{1\rho}$-parameters confirms the previous results. Furthermore, it allows us to evidence that the dipolar interaction governs the relaxation, at variance with what was generally accepted.

Unusual behaviour also arises for the T_2-parameters in the same temperature range as for T_1 and $T_{1\rho}$. To account for this behaviour, which is also observed in conductivity, we suggest a change in the slow motion: below 200 K the slow motion corresponds to Li^+-ion hops between cages through the bottleneck in the (a, b) plane, while above this temperature and owing to phonons, the Li^+ ions hop in the three directions. The change in dimension from 2D (in the low-temperature range) to 3D (in the high-temperature range) is also corroborated by the ratio of the activation energies in the two domains, i.e. 1.5.

References

[1] Belous A G, Novitskaya G N, Polyanetskaya S V and Gornikov Y I 1987 *Zh. Neorg. Khim.* **32** 283
[2] Inaguma Y, Chen L, Itoh M, Nakamura T, Ushida T, Ikuta H and Wakihara M 1993 *Solid State Commun.* **86** 689
[3] Robertson A D, Garcia Martin S, Coats A and West A R 1995 *J. Mater. Chem.* **5** 1405
[4] Fourquet J L, Duroy H and Crosnier-Lopez M P 1996 *J. Solid State Chem.* **127** 283
[5] Mazza D, Ronchetti S, Bohnké O, Duroy H, and Fourquet J L 2001 *Solid State Ion.* submitted
[6] Bohnké O, Duroy H, Fourquet J L, Ronchetti S and Mazza D 2001 *Solid State Ion.* submitted
[7] Inaguma Y, Chen L, Itoh M and Nakamura T 1994 *Solid State Ion.* **70/71** 196
[8] Itoh M, Inaguma Y, Jung W H, Chen L and Nakamura T 1994 *Solid State Ion.* **70/71** 203
[9] Bohnké O, Bohnké C and Fourquet J L 1996 *Solid State Ion.* **91** 21
[10] Katsumata T, Matsui Y, Inaguma Y and Itoh M 1996 *Solid State Ion.* **86/88** 165
[11] Inaguma Y and Itoh M 1996 *Solid State Ion.* **86/88** 257
[12] Bohnké O and Emery J 2001 *Chem. Mater.* submitted
[13] Zerouale A, Cros B, Deroide B and Ribes M 1988 *Solid State Ion.* **28–30** 1317
[14] Fan J, Marzke R F, Sanchez E and Angell C A 1994 *J. Non-Cryst. Solids* **172–4** 1178
[15] Emery J, Buzaré J Y, Bohnké O and Fourquet J L 1997 *Solid State Ion.* **99** 41
[16] Bohnké O, Emery J, Veron A, Fourquet J L, Buzaré J Y, Florian P and Massiot D 1998 *Solid State Ion.* **109** 25
[17] Emery J, Bohnké O, Fourquet J L, Buzaré J Y, Florian P and Massiot D 1999 *J. Phys.: Condens. Matter* **11** 1
[18] Leon C, Lucia M L, Santamaria J, Paris M A, Sanz J and Varez A 1996 *Phys. Rev.* B **54** 184
[19] Leon C, Santamaria J, Paris M A, Sanz J, Ibarra J and Torres L M 1997 *Phys. Rev.* B **56** 5302
[20] Massiot D, Thiele H and Germanius A 1994 *Bruker Rep.* **43** 140
[21] Alonso J A, Sanz J, Santamaria J, Leon C, Varez A and Fernandez-Diaz M T 2000 *Angew. Chem. Int. Edn Engl.* **39** 619
[22] Hirakoso Y, Harada Y, Kuwano J, Saito Y, Ishikawa Y and Eguchi T 1999 *Key Eng. Mater.* **169–70** 209
[23] Paris M A, Sanz J, Leon C, Santamaria J, Ibarra J and Varez A 2000 *Chem. Mater.* **12** 1694
[24] Petit D and Korb J P 1988 *Phys. Rev.* B **37** 5761
[25] McLachlan A D 1964 *Proc. R. Soc.* A **280** 271
[26] Hubbard P S 1970 *J. Chem. Phys.* **53** 985
[27] Bull T E 1972 *J. Magn. Reson.* **8** 344
[28] Werbelow L G 1979 *J. Chem. Phys.* **70** 5381
[29] Richards P M 1979 *Physics of Superionic Conductors (Springer Topics in Current Physics)* (Berlin: Springer) p 141
[30] Andrew E R and Tunstall D P 1961 *Proc. Phys. Soc.* **78** 1
[31] Korb J P, Private communication
[32] Korringa J 1950 *Physica* **16** 601